PHYSICAL REVIEW B VOLUME 47, NUMBER 14 1 APRIL 1993-II

Effective dielectric response of a composite with aligned spheroidal inclusions

Rubén G. Barrera
Instituto de Física, Universidad Nacional Autónoma de México, Apartado Postal 20-364, 01000 México, Distrito Federal, Mexico

Jairo Giraldo
Departamento de Física, Universidad Nacional de Colombia, Bogotá, Colombia

W. Luis Mochán
Laboratorio de Cuernavaca, Instituto de Física, Universidad Nacional Autónoma de México, Apartado Postal 139-8, 62190 Cuernavaca, Morelos, Mexico

(Received 26 September 1991; revised manuscript received 17 December 1992)

The effective dielectric response ϵ_M of a composite with aligned spherodial inclusions is calculated. Using the dipolar and the mean-field approximation (MFA) an analytical expression for ϵ_M as a functional of the two-particle distribution function $\rho^{(2)}$ is obtained. It is shown that previous expressions reported in the literature correspond to different choices of $\rho^{(2)}$, thus, clarifying the origin of their discrepancies. The theory is further extended beyond the MFA by including the dipolar fluctuations through a renormalization of the polarizability tensor of the inclusions. The absorption peaks are diminished and broadened by the spatial disorder, which also yields an easily identified coupling among electromagnetic modes with perpendicular polarizations.

I. INTRODUCTION

The study of the linear electromagnetic response of composite materials has attracted the attention of many researchers since the beginning of electrodynamics.[1] This interest has been recently renewed due to the development of new theoretical methods for dealing with disordered systems[2] and also to the potential applications of composite materials in solar energy conversion,[3] earth sciences,[4] biology,[5] and other fields.[6] It has been established by now that the dielectric response of composites is very sensitive to the topology of its microstructure. Here we restrict ourselves to composites prepared as small inclusions, much smaller than the wavelength of the incoming electromagnetic radiation, embedded in an otherwise homogeneous, isotropic host material. The problem to be considered here is the calculation of the macroscopic dielectric response ϵ_M in terms of the dielectric responses of its constituents and the statistical properties of the distribution of inclusions. Although the results obtained so far for spherical monodispersed inclusions cover a wide range of methods and approximations,[7] extensions to nonspherical inclusions have been restricted, almost entirely, to the mean-field approximation (MFA). Even in this case the problem has not been thoroughly examined.

For a system with spherical inclusions, an early expression for ϵ_M which appears in the literature was derived by Maxwell Garnett.[8] The Maxwell Garnett theory (MGT) is a mean-field theory equivalent to the celebrated Clausius-Mossotti-Lorenz-Lorentz relation.[9]. The only statistical property of the system required by this theory is the fraction of the volume occupied by the inclusions. In the popular Lorentz method (LM) for deriving the MFA,[10] one considers a fictitious spherical cavity in the system, known as the Lorentz sphere, which is centered at a reference inclusion. The MFA is obtained when the contribution to the local field due to the other inclusions contained in the cavity is neglected and the contribution from those outside the cavity is taken in the continuous limit.

Here we consider the study of shape effects in ϵ_M for systems with aligned nonspherical inclusions. In this case the macroscopic physical properties of the system are anisotropic and the effective dielectric response will be described by a second rank tensor $\underline{\epsilon}_M$ with its principal axes along the principal axes of the spheroids.

Our objective is the calculation of $\underline{\epsilon}_M$ in terms of the dielectric functions of its constituents and the statistical properties of the distribution of spheroids. This old problem was stated already in Maxwell's treatise[11] in connection with a proposal of a microscopic model for explaining the birefringence of crystals. In the dilute limit, when the spheroids are so far apart from each other that there is no interaction among them, the effective dielectric response $\underline{\epsilon}_M$ depends linearly on the polarizability tensor $\underline{\alpha}$ of an isolated spheroid. The fields induced in an isolated spheroid by a slowly varying (in space) external field are well known[12] and the principal components of $\underline{\alpha}$ are given by closed analytical expressions.[13]

As the volume fraction of the aligned spheroidal inclusions increases, the interaction among themselves through the local induced fields has to be taken into account in the calculation of the dielectric response. This was done by Wiener[14] as early as 1912 within a mean-field approximation. His expression for $\underline{\epsilon}_M$ was rediscovered in 1953 by Bragg and Pippard[15] and in 1973 by Cohen *et al.*,[16] who extended the LM to the case of ellipsoids by neglecting the near field due to the inclusions within an ellipsoidal fictitious cavity with the same eccentricity as the embedded particle. However, an alternative expres-

sion for $\underline{\epsilon}_M$ was also proposed by Galeener[17] which chose instead a spherical fictitious cavity. Both of these expressions, as well as a third alternative, have been rederived through the random-unit-cell method.[18,19]

The only criteria to decide which of these expressions is the correct one has been, so far, to compare their asymptotic behavior in the limits of extreme eccentricity ($e \to 1$), flat dishes, and needles, where the exact result is known.[15] Obviously, this criteria is unsatisfactory. As an alternative to the phenomenological models above, here we solve a microscopic model. We consider a composite consisting of a homogeneous, isotropic matrix with aligned identical spheroidal inclusions. We show below that even within the MFA, for nonspherical inclusions $\underline{\epsilon}_M$ depends on the microstructure of the sample, as characterized by its two-particle distribution function, besides the volume fraction. The three expressions above are correct; they are special cases of the MFA, but they correspond to three different choices of the two-particle distribution functions. The reason one of them fails in the $e \to 1$ limit is also discussed.

After developing the MFA, we improve on taking into account the fluctuations in the induced dipole moments. To this end we introduce a renormalized polarizability tensor $\underline{\alpha}^*$, in a similar way as it was done for the case of spherical inclusions.[20] We show that the two electromagnetic resonances of a single spheroid, corresponding to polarization along its principal axes, appear shifted and asymmetrically broadened in the absorption spectra of the composite due to the field fluctuations. Furthermore, the fluctuations also couple these two modes, even when the external field is along a principal direction, yielding two absorption peaks instead of the single peak predicted by the MFA.

A very closely related problem is that of dichroism in nematic liquid crystals. In this case, instead of inclusions, we have aligned anisotropic polarizable molecules. There have been many investigations of the anisotropy of the local field in these systems.[21,22] So far, the theoretical approaches[22] have been phenomenological extensions of the LM which do not take properly into account the role played by the distribution functions nor by the field fluctuations.

The structure of the paper is as follows: In Sec. II, we present the theory, starting with the derivation of the MFA along with some comments about its comparison with earlier results. Then we present a formalism which takes us beyond the MFA. The results are presented and discussed in Sec. III and Sec. IV is devoted to conclusions.

II. THEORY

Let us consider a system of $N \gg 1$ aligned identical polarizable spheroids with semiaxes a and $b=c$, polarizability components α^γ (in principal γ axis) with centers located at random positions $\{\mathbf{R}_i\}$ within an otherwise homogeneous, isotropic matrix characterized by a dielectric function ϵ_h. The system is excited by a spatially dependent external electric field $\mathbf{E}_{ex}$ with a wave vector $q \ll 1/a, 1/b$ and oscillating with frequency ω. By external field we mean that produced by charge and current densities introduced to perturb the system, as opposed to the field induced by polarization or conduction charges. Setting our coordinate system along the principal axis of the polarizability tensor of the aligned spheroids, with the z axis along the axis of symmetry, the induced dipole moment $\mathbf{p}_i$ of the ith spheroid obeys

$$p_i^\gamma = \alpha^\gamma \left[E_{0i}^\gamma + \sum_{j,\delta} s_{ij}^{\gamma\delta} p_j^\delta \right] , \tag{1a}$$

where the superscripts $\gamma,\delta = x,y,z$ indicate Cartesian components and $\mathbf{E}_{0i}$ is the electrical field at $\mathbf{R}_i$ in the absence of the spheroids. We remark that $\mathbf{E}_{0i}$ and $\mathbf{E}_{ex,i}$ differ due to the polarization of the host. The unscreened interaction tensor $s_{ij}^{\gamma\delta}$ relates the γ component of the electric field at $\mathbf{R}_i$ produced by all the charges induced at the surface of a polarized spheroid with dipole moment $\mathbf{p}_j^\delta$ at $\mathbf{R}_j$. This induced field is dipolar only at large distances; the explicit expressions for $s_{ij}^{\gamma\delta}$ are given in Appendix A. The principal components of the polarizability tensor of a single spheroidal inclusion, in cgs units, are given by[13]

$$\alpha^\gamma = \tfrac{1}{3} a b^2 \frac{\epsilon_m - \epsilon_h}{L_\gamma \epsilon_m + (1-L_\gamma)\epsilon_h} , \tag{1b}$$

where ϵ_m and ϵ_h are the dielectric functions of the inclusions and host, respectively, and L_γ are the depolarization factors of a spheroid which fulfill $\sum_\gamma L_\gamma = 1$. For a prolate (oblate) spheroid, that is when $a > b$ ($a < b$), the depolarization factor along the symmetry axis is given by[13]

$$L_z(e) = \begin{cases} \dfrac{1}{g^2(e)} \left[\dfrac{1}{2e} \ln \dfrac{1+e}{1-e} - 1 \right] & (P) , \\ \dfrac{1}{e^2} \left[1 - \dfrac{1}{g(e)} \tan^{-1} g(e) \right] & (O) , \end{cases} \tag{1c}$$

and

$$L_x = L_y = \tfrac{1}{2}(1 - L_z) , \tag{1d}$$

where

$$e = (1 - r_<^2 / r_>^2)^{1/2} \tag{1e}$$

is the eccentricity, $r_<$ ($r_>$) is the smaller (larger) of the semiaxes, and

$$g(e) = e/(1-e^2)^{1/2} . \tag{1f}$$

Hereafter (P) or (O) following any expression refers to prolate or oblate spheroids, respectively. Notice that both the host and inclusion contribute to the charge induced at the surface of a given spheroid, and both contributions are included in the polarizability, as given by Eq. (1b). It is for this reason that we take $s_{ij}^{\gamma\delta}$ as the *unscreened* interaction tensor.

Due to the long range of $s_{ij}^{\gamma\delta}$, the evaluation of sums such as those in Eq. (1a) might yield ill-defined integrals and shape-dependent intermediate results. In order to circumvent these difficulties, here we adopt the same pro-

cedure used in Ref. 20: First we chose a longitudinal external field with a small but finite wave vector $\mathbf{q}$ along a principal direction of the system, such that $1/q$ is much smaller than the size L of the system. This choice eliminates the dependence on the shape of the sample and, furthermore, it allows the identification of the external field with the macroscopic displacement field.[20] This can be shown as follows: (i) The external longitudinal field equals the longitudinal projection of the displacement field $\mathbf{D}^L$ since both have identical divergence and a null curl. (ii) Since $\mathbf{E}_{ex}$ is longitudinal and along a principal axis, then $\mathbf{D}\|\mathbf{E}_{ex}\|\mathbf{q}$ at distances from the boundary of the sample much larger than the inverse wave vector $1/q$. (iii) Then, in the thermodynamic limit ($L\to\infty$), $\mathbf{D}=\mathbf{D}^L$ is longitudinal and therefore $\mathbf{D}=\mathbf{E}_{ex}$. As a final step, we take the $q\to 0$ limit, that is, one keeps only the lowest-order term in the small quantities qa and qb.

The choice of a longitudinal external field is just a matter of convenience; a transverse external field would be related in a different way to the macroscopic fields, but it would convey the same components of the dielectric tensor when referred to a fixed reference frame since the dielectric response is regular in the $\mathbf{q}\to 0$ limit.

The longitudinal external field can be written as

$$\mathbf{E}_{ex}(\mathbf{r},t)=E_{ex}\hat{\mathbf{q}}e^{i(\mathbf{q}\cdot\mathbf{r}-\omega t)}\ , \tag{2}$$

where $\hat{\mathbf{q}}=\mathbf{q}/q$ and $\mathbf{r}$ and t are the space and time coordinates, respectively. In an ordered system the polarization p_i would have an oscillatory dependence on i, $\exp(i\mathbf{q}\cdot\mathbf{R}_i)$, inherited from that of the external field. We get rid of this trivial dependence in this and subsequent equations by introducing the transformation

$$P_i^\gamma=p_i^\gamma e^{-i(q\cdot\mathbf{R}_i-\omega t)}\ . \tag{3}$$

Here we write P_i^γ instead of P^γ since in the system under consideration there is a further dependence on i due to disorder. When $\mathbf{E}_{0i}=\mathbf{E}_{ex,i}/\epsilon_h$ is substituted into Eq. (1), with $\mathbf{E}_{ex}$ and $\hat{\mathbf{q}}$ along a particular but arbitrary principal direction ζ, one gets

$$P_i^\gamma=\alpha^\gamma\left[E_{ex}\delta_{\gamma\zeta}/\epsilon_h+\sum_{j,\delta}S_{ij}^{\gamma\delta}P_j^\delta\right]\ , \tag{4a}$$

where we write $\hat{q}^\gamma$ as a Kronecker's delta function $\delta_{\gamma\zeta}$, and we introduced the transformed, q-dependent interaction

$$S_{ij}^{\gamma\delta}=S_{ij}^{\gamma\delta}(\mathbf{q})\equiv s_{ij}^{\gamma\delta}e^{-iqR_{ij}^\zeta}\ , \tag{4b}$$

where $R_{ij}\equiv\mathbf{R}_i-\mathbf{R}_j$.

Since the longitudinal external field lies along the principal direction ζ, the macroscopic electric field $\mathbf{E}(\mathbf{r},t)=E\hat{\mathbf{q}}e^{iqR^\zeta-\omega t}$, as well as all the other pertinent macroscopic fields such as the polarization density and the displacement field, lie along ζ. Therefore,

$$E=\frac{E_{ex}}{\epsilon_h}-4\pi n\langle P\rangle\ , \tag{5}$$

where n is the number density of the inclusions, $\langle\cdots\rangle$ denote ensemble average, and $\langle P_i^\gamma\rangle=\langle P\rangle\delta^{\gamma\zeta}$ is independent of i. The first term on the RHS of Eq. (5) takes account of the host depolarization in the absence of the inclusions, and the second one is the longitudinal depolarization due to the inclusions themselves.

Recalling that the macroscopic dielectric tensor $\underline{\epsilon}_M$ is defined through $\mathbf{D}=\underline{\epsilon}_M\mathbf{E}$, and the longitudinal field $\mathbf{E}_{ex}$ equals the macroscopic displacement field $\mathbf{D}$, we obtain from Eq. (5)

$$\epsilon_h/\epsilon_M^\zeta(q,\omega)=1-4\pi\epsilon_h\chi_{ex}^\zeta(q,\omega)\ , \tag{6a}$$

where $\chi_{ex}^\zeta(q,\omega)$ is a principal component of the external susceptibility tensor defined through

$$n\langle P\rangle=\chi_{ex}^\zeta(q,\omega)E_{ex}\ . \tag{6b}$$

For long wavelengths, the local macroscopic dielectric response $\underline{\epsilon}_M(\omega)$ is finally obtained through the limit

$$\underline{\epsilon}_M^\zeta(\omega)=\lim_{q\to 0}\underline{\epsilon}_M^\zeta(q,\omega)\ . \tag{7}$$

When the procedure above is repeated with ζ along each of the two remaining principal directions, we obtain the full dielectric tensor $\underline{\epsilon}_M(\omega)$.

A. The mean-field approximation

In the MFA the disorder-induced fluctuations of the dipolar moments are neglected, thus one takes $P_i^\gamma=\langle P\rangle\delta^{\gamma\zeta}$. Since the average of the off-diagonal Cartesian components of $S_{ij}^{\gamma\delta}$ vanish, from Eq. (4a) we obtain that the average dipole moment obeys

$$\langle P\rangle=\alpha^\zeta\left[E_{ex}/\epsilon_h+\left\langle\sum_j S_{ij}^{\zeta\zeta}\right\rangle\langle P\rangle\right]\ , \tag{8}$$

which can be trivially solved for $\langle P\rangle$. Therefore, combining Eqs. (7), (6), and (8), one obtains readily an expression for the effective dielectric response,

$$\frac{\epsilon_M^\zeta-\epsilon_h}{\mathcal{L}_\zeta\epsilon_M^\zeta+(1-\mathcal{L}_\zeta)\epsilon_h}=3f\tilde{\alpha}^\zeta=f\frac{\epsilon_m-\epsilon_h}{L_\gamma\epsilon_m+(1-L_\gamma)\epsilon_h}\ , \tag{9}$$

where

$$4\pi n(\mathcal{L}_\zeta-1)\equiv\lim_{q\to 0}\left\langle\sum_j S_{ij}^{\zeta\zeta}\right\rangle=\lim_{q\to 0}\left\langle\sum_j s_{ij}^{\zeta\zeta}\exp(-iqR_{ij}^\zeta)\right\rangle$$

is the longitudinal average of the particle-particle interaction. $\mathcal{L}_\zeta$ is independent of i due to the homogeneity of the ensemble. Here $f=4\pi nab^2/3$ is the volume fraction of spheroids and $\tilde{\alpha}^\gamma=\alpha^\gamma/ab^2$.

The average interaction is now calculated as[20]

$$\mathcal{L}_\zeta-1=\lim_{q\to 0}\frac{1}{4\pi}\int s^{\zeta\zeta}(\mathbf{R})e^{-iqR^\zeta}\rho^{(2)}(\mathbf{R})d^3R\ , \tag{10}$$

which contains the two-particle distribution function $\rho^{(2)}(\mathbf{R})$ of the spheroids. In the very special case of spherical inclusions with a spherically symmetric distribution function, $\mathcal{L}^\zeta=\frac{1}{3}$, independent of $\rho^{(2)}(R)$,[20] and ϵ_M depends only on the volume fraction of the spheres. On the other hand, for spheroidal inclusions $\underline{\epsilon}_M$ becomes a functional of $\rho^{(2)}(\mathbf{R})$ *even* in the MFA.

In the rest of this section we will illustrate the dependence of $\underline{\epsilon}_M$ on $\rho^{(2)}(\mathbf{R})$ by first considering, in $\rho^{(2)}(\mathbf{R})$, only the hole correction (HC): $\rho^{(2)}(\mathbf{R})$ takes the value 0 within a small correlation hole that surrounds the inclusion and the value 1 outside. If the hole is given by the volume excluded by hard aligned spheroids, that is, a similar spheroid of semiaxes $2a$ and $2b=2c$, then it can be shown (see Appendices B and C) by direct integration of Eq. (10) that

$$\mathcal{L}_\xi = L_\xi \ , \tag{11}$$

where $\mathcal{L}_\xi$ is the depolarization factor of the inclusions given in Eqs. (1c) and (1d). In this case Eq. (9) is exactly the same expression as the one derived in Ref. 16 using the Lorentz method with a spheroidal fictitious cavity with the same eccentricity as the inclusions. On the other hand, if the correlation hole is spherical, then one obtains Galeener's expression[17] which was originally derived with the LM but with a spherical fictitious cavity instead of a spheroidal one. Also, the expression derived by the method of Niklasson and Grandqvist[18] using as a random unit cell a spheroid with a cofocal spheroidal coating, can be derived directly from Eq. (9); in this case the exclusion hole in $\rho^{(2)}_{\rm HC}$ is a spheroid cofocal to the inclusion. Moreover, for any spheroidal correlation hole $\mathcal{L}_\xi$ are simply the depolarization factors of the *hole,* as shown in Appendices B and C.

Therefore, we have shown that the three results mentioned above are correct within the MFA, but they correspond to different systems characterized by three different distribution functions. Among them, it is only Galeener's expression that does not hold in the $e \to 1$ limit. However, we point out that in this case, the radius of the spherical correlation hole must be larger than the largest axis to avoid interpenetration. Thus, the excentricity is bounded by $e^2 < 1-f$ ($e^2 < 1-f^2$) for prolate (oblate) spheroids, and the $e \to 1$ limit has no physical realization except in the trivial $f=0$ case.

It is interesting to notice that in the three cases discussed above, the shape of the fictitious cavity in the LM or the shape of the coating in the random-unit-cell method is related directly to the microscopic shape of the exclusion hole in the two-particle distribution function. This is not surprising because performing the MFA together with a HC distribution function is equivalent to replacing the exterior of the correlation hole with a continuous, uniformly polarized medium, which is the basis of the previous phenomenological procedures. However, our microscopic approach clarifies the ambiguity in the choice of the cavity. Furthermore, our theory is capable of accounting for the structure which would appear in the two-particle distribution function of any real system. We remark that our theory does not require a cavity, as it can be applied to systems with an arbitrary $\rho^{(2)}$, and that for some conceivable systems our MFA result will not be equivalent to a system described by any spheroidal cavity, as $\mathcal{L}_\gamma$ obtained from Eq. (10) need not obey the depolarization factors' sum rule [Eq. (1d)].

We also remark that, as shown in Appendix B, within the MFA and for a spheroidal correlation hole, and more generally, for any two-particle distribution function with spheroidal symmetry, we obtain the correct results when we substitute the exact interaction $s_{ij}^{\gamma\delta}$ by the dipole-dipole interaction tensor

$$t_{ij}^{\gamma\delta} = (1-\delta_{ij})\partial_i^\gamma \partial_j^\delta (1/R_{ij}) \tag{12}$$

in Eq. (1a). This is due to the vanishing of the angular average of all higher multipolar fields when integrated over the surface of a spheroid.

Finally, before closing this section, we want to add that the proper choice of the two-particle distribution function will be determined by the specific characteristic of the samples to be examined and the best thing would be to extract $\rho^{(2)}$ directly from the samples. Nevertheless, a calculation of ϵ_M^ξ for the hard-spheroid models, with a better approximation for $\rho^{(2)}(\mathbf{R})$ than the hole correction, will be welcomed.

B. Beyond the mean-field approximation

Following the procedure of Ref. 20 we now introduce a renormalized polarizability tensor with principal components $\alpha^{*\gamma}$ through the approximate equation

$$P_i^\gamma = \alpha^{*\gamma}\left[E_{\rm ex}\delta_{\gamma\xi}/\epsilon_h + \sum_j S_{ij}^{\gamma\xi}\langle P\rangle^\xi\right] , \tag{13}$$

where, as before, ξ indicates the direction of the longitudinal external field which is taken along an arbitrary principal direction. The value of $\alpha^{*\gamma}$ will be chosen below by demanding a consistency condition among Eqs. (13) and (4). The term within parenthesis in Eq. (13) is the local field that would be produced if the induced dipoles had no fluctuations. This field fluctuates due to the disorder in the positions $\mathbf{R}_{ij}$ and therefore in the interactions $S_{ij}^{\gamma\xi}$. The fluctuations in the true local field due to the fluctuations in the induced dipoles themselves are incorporated approximately through the renormalized polarizability.

Taking now the ensemble average of Eq. (13) one obtains an equation exactly similar to Eq. (8) but with α^γ replaced by $\alpha^{*\gamma}$. Therefore, the macroscopic dielectric response is given by

$$\frac{\epsilon_M^\xi - \epsilon_h}{\mathcal{L}_\xi \epsilon_M^\xi + (1-\mathcal{L}_\xi)\epsilon_h} = 3f\tilde{\alpha}^{*\xi} , \tag{14}$$

where $\tilde{\alpha}^{*\xi} = \alpha^{*\xi}/ab^2$.

The problem is then the calculation of $\tilde{\alpha}^{*\gamma}$, for which we also follow the method proposed in Ref. 20. First one substitutes the expression for P_j^γ, as given by Eq. (13), into the right-hand side of Eq. (4a) and then takes the ensemble average of the resulting equation. One obtains

$$\frac{\alpha^{*\gamma}}{\alpha_\gamma} = 1 + \alpha^{*\gamma}\sum_\delta \alpha^{*\delta}\lim_{q\to 0}\left[\left\langle \sum_{jk} S_{ij}^{\gamma\delta}S_{jk}^{\delta\gamma}\right\rangle - \left\langle \sum_j S_{ij}^{\gamma\delta}\right\rangle^2\right] . \tag{15}$$

The term within square brackets in this equation corresponds to the variance of the interaction. Clearly, in the absence of fluctuations this variance would be zero and

the renormalized and bare polarizability would coincide. We remark that the $q \to 0$ limit of each of the terms within the square brackets depends on the direction of $\mathbf{q}$, but this dependence disappears from the variance. This statement is equivalent to the absolute convergence and shape independence of the integrals that correspond to the averages in Eq. (15) for a constant external field, as discussed in Ref. 23. Therefore, the particular direction ζ plays no special role from here on.

Equation (15) constitutes a system of two coupled second-order algebraic equations for $\tilde{\alpha}^{*z}$ and $\tilde{\alpha}^{*x}=\tilde{\alpha}^{*y}$ whose coefficients depend on the fluctuations of the interaction tensor. The solution of this system of equations is substituted into Eq. (14) to obtain the sought after macroscopic dielectric response. To perform this calculation we require the two- and three-particle distribution functions as well as the bare polarizability of the inclusions. An application to a specific system will be developed in the next section. To abbreviate, in the following we will refer to the procedure described in the present section as RPT which stands for renormalized polarizability theory.

III. RESULTS

In this section we apply the theory above to a system of metallic spheroidal inclusions embedded in dispersionless gelatin. We choose for the inclusions a Drude dielectric function

$$\epsilon_m = 1 - \omega_p^2/\omega(\omega + i/\tau) , \tag{16}$$

where ω_p is the plasma frequency and τ the electronic relaxation time. For gelatin we take $\epsilon_h = 2.37$ independent of frequency.

If we restrict ourselves to the low-density regime, we can assume that the three-particle distribution function $\rho^{(3)}(\mathbf{R}_1,\mathbf{R}_2,\mathbf{R}_3)$, which is required for the evaluation of $\lim_{q\to 0}\langle \sum_{jk} S_{ij}^{\gamma\delta} S_{jk}^{\delta\gamma} \rangle$, can be approximated by

$$\rho^{(3)}(\mathbf{R}_1,\mathbf{R}_2,\mathbf{R}_3) \simeq \rho^{(2)}(R_{12})\rho^{(2)}(R_{23}) . \tag{17}$$

In this case Eq. (15) becomes

$$\frac{\tilde{\alpha}^{*\gamma}}{\tilde{\alpha}^{\gamma}} = 1 + \tfrac{1}{4}\tilde{\alpha}^{*\gamma} \sum_{\delta} f^{\gamma\delta}\tilde{\alpha}^{*\delta} , \tag{18}$$

where coefficients $f^{\gamma\delta}$ are given by

$$\tfrac{1}{4} f^{\gamma\delta} = (ab^2)^2 \left\langle \sum_j S_{ij}^{\gamma\delta} S_{ji}^{\delta\gamma} \right\rangle , \tag{19}$$

and they account for the self-interaction of the ith inclusion mediated by the other jth inclusions. We further assume that $\rho^{(2)}$ is given by the hole correction with a spheroidal correlation hole with the same excentricity as the inclusions.

Substituting the expressions for $s_{ij}^{\gamma\delta}$ given in Eq. (A3) into Eq. (19), one obtains, after some algebra,

$$f^{\gamma\delta} = 54 f \eta_0 (\eta_0^2 \mp 1) C^{\gamma\delta} Q^{\gamma\delta} , \tag{20}$$

where $\eta_0 = 1/e$ ($\eta_0 = 1/g(e)$) is the value of the spheroidal coordinate which defines the surface of the actual inclusion, and we chose the upper (lower) sign for prolate (oblate) spheroids. Here, $C^{\gamma\delta}$ are constants whose values are given in Appendix D and $Q^{\gamma\delta}$ is a set of quadratures whose derivation is displayed also in Appendix D.

In the case of extreme eccentricity $e \to 1$, the parameter η_0 becomes 1 (0) for prolate (oblate) spheroids. From the prefactor in Eq. (20), $f^{\gamma\delta} \to 0$ in this limit. Thus, the effect of the fluctuations disappears in a system composed of sharp needles (flat dishes) and our theory yields the same asymptotic behavior as the MFA, which for our choice of $\rho^{(2)}$ is the correct one, as pointed out before.

The calculation of $\underline{\epsilon}_M$ is performed in the following way: first we calculate, by numerical integration, the coefficients $f^{\gamma\delta}$, given in Eq. (20) and then we solve (also numerically) the system of coupled quadratic equations given in Eq. (18). The results obtained for $\tilde{\alpha}^{*\gamma}$ are then substituted into Eq. (14) in order to get ϵ_M^{γ}.

In Figs. 1 and 2 we show $\mathrm{Im}\epsilon_M^{\gamma}$ ($\gamma = x,z$) calculated within RPT, as a function of ω/ω_p for a system of prolate spheroidal metallic inclusions with eccentricity $e = 0.5$ and 0.9, respectively, a lifetime $\tau = 1000/\omega_p$ and a filling fraction $f = 0.01$. We also show the corresponding calculations in the MFA, which display a single resonance peak for each direction γ. These peaks originate from the surface plasmon resonances of an isolated spheroid. The resonance that occurs at a higher (lower) frequency corresponds to polarization along the short (long) axis of the spheroid, as is also the case for isolated spheroids, either oblate or prolate. Both peaks are red shifted with respect to those of a single particle due to the interactions, but their width ($1/\tau$) remains the same. This width is due only to dissipation since in the absence of fluctuations there is only one optically active mode in the $q \to 0$ limit. On the other hand, the corresponding peaks in RPT are asymmetrically broadened. The origin of

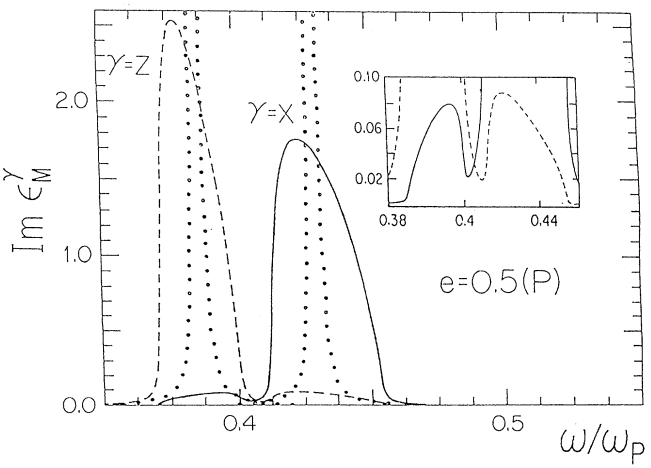

FIG. 1. Imaginary part of the principal components of the macroscopic dielectric response ϵ_M^{γ} as a function of the normalized frequency ω/ω_p for a composite made up of prolate inclusions aligned along the Z axis. The volume fraction is $f = 0.01$, the eccentricity $e = 0.5$, and the dissipation constant is $\tau = 1000/\omega_p$. The dotted line was calculated using the MFA and the solid line using RPT. The inset shows an amplified region of the same figure.

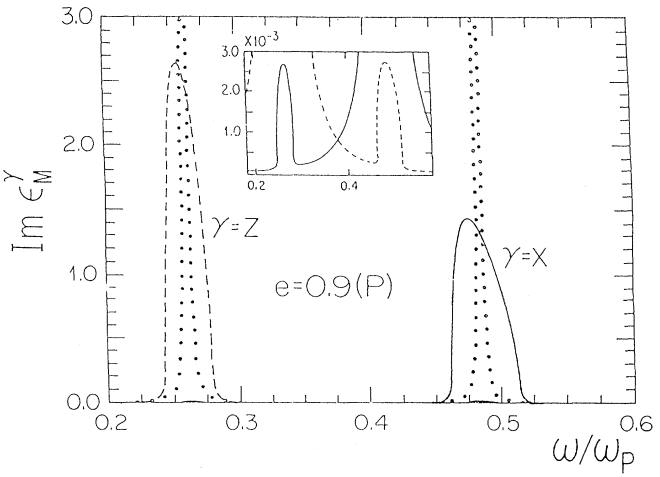

FIG. 2. Same as Fig. 1 but with a larger eccentricity $e=0.9$.

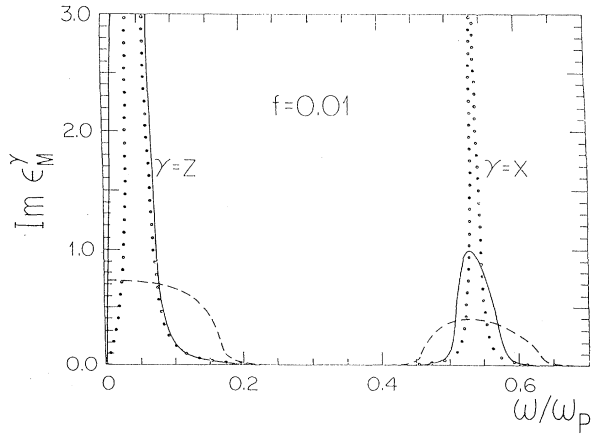

FIG. 4. Same as Fig. 1 but with a much larger eccentricity $e=0.99$. The results of RPT using a dipolar interaction tensor are also shown as the dashed curve.

these broadenings is the excitation of manifold modes which become optically active in a disordered system, whose spectrum covers a continuous range of frequencies. This range is quite unsensitive to dissipation. It is to illustrate this point that we chose such a large lifetime.

It can also be seen in Figs. 1 and 2 that for each direction γ, the RPT results show a small secondary peak at a frequency which corresponds to the primary peak of the unequivalent direction $\bar{\gamma}$. This can be interpreted as the coupling between electromagnetic modes with polarizations along the γ and $\bar{\gamma}$ directions, and originates from the nondiagonal elements of the variance of $S_{ij}^{\gamma\delta}$ in Eq. (15). The presence of the secondary peak, which is absent in the MFA, is an unequivocal signature of the fluctuations, in contrast to the disordered-induced broadening which might be confused with the broadening due to dissipation within an individual inclusion. In the case of spheres, this coupling also exists, but the modes with mutually perpendicular directions cannot be discriminated since they have the same frequencies. In general, the strength of this mode coupling diminishes as the eccentricity increases, as can be seen by comparing Figs. 1 and 2. In the limit $e\to 1$ the coupling vanishes since in this case the fluctuations disappear.

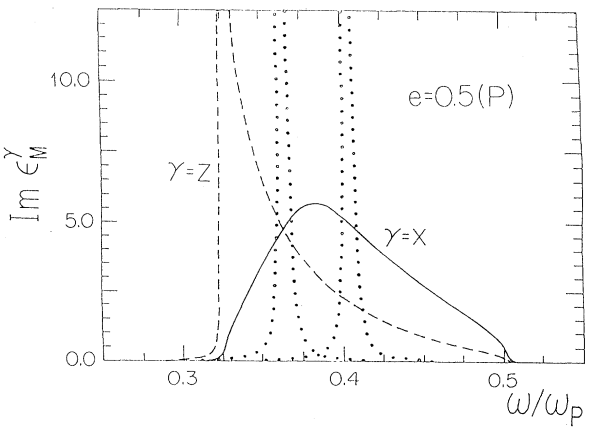

FIG. 3. Same as Fig. 1 but with a larger filling fraction $f=0.1$.

Figure 3 shows the result of a similar calculation as in Fig. 1 but for a larger volume fraction $f=0.1$. In this case, for each direction $\gamma=x,z$, the primary and secondary peaks are so disorder broadened that they overlap and can no longer be individually resolved as in the previous figures.

The main peaks in our calculations are always red shifted with respect to the corresponding ones in the MFA. However, as the eccentricity increases, the location of their maxima approaches the corresponding ones in MFA, and in the limit $e\to 1$ both calculations coincide. In Fig. 4, we show how the results of RPT approach those of the MFA; to this end we chose a large eccentricity $e=0.99$. We also show the results of a RPT calculation using the dipolar interaction tensor $t_{ij}^{\gamma\delta}$ [Eq. (12)] instead of the exact one $s_{ij}^{\gamma\delta}$ [Eq. (A3)] (the corresponding parameters $f^{\gamma\delta}$ are calculated in Appendix E). It can be clearly seen from this figure that, while the latter calculation does approach the MFA, there are substantial deviations in the former case, which does not attain the correct MFA limit when $e\to 1$. Nevertheless, we remark that these two RPT calculations depart from each other only at high eccentricities. Although we have only shown results for prolate inclusions, we have obtained similar results for the oblate case.

IV. CONCLUSIONS

In this paper, we have calculated the effective dielectric response ϵ_M of a composite, prepared as a homogeneous, isotropic matrix with aligned spheroidal inclusions. Since most of the work in this field has been done with spherical inclusion, the main purpose here was to explore the effects of a nonspherical shape. The calculations were performed assuming that each inclusion was uniformly polarized; an assumption which is valid in the low-

density regime. First, we obtained, in the mean-field approximation, an explicit analytic expression for $\underline{\epsilon}_M$ in terms of the dielectric functions of the matrix and the inclusions and as a functional of their two-particle distribution function $\rho^{(2)}$. By choosing specific models for the correlations in $\rho^{(2)}$, we obtained different expressions which were derived previously using phenomenological approaches, thus clarifying the origin of their discrepancies. We also discussed the inadequacy of the $e \to 1$ limit as a criterion for judging their validity. However, our approach may incorporate more realistic forms of the correlations, for which different results will be obtained. This means that one requires more microstructural information besides the volume fraction of inclusions in order to apply an effective medium theory even in the MFA.

We extend the mean-field theory by taking account of the field fluctuations through the introduction of a renormalized polarizability tensor. The calculations of this tensor now requires information not only about $\rho^{(2)}$ but also about $\rho^{(3)}$. We present results valid in the low-density regime where $\rho^{(3)}$ is approximated by a product of $\rho^{(2)}$ and where multipolar effects can be neglected. Nevertheless, this factorization approximation is not demanded by the theory. At high densities, where the approximation is no longer valid, one can still use the theory if one has enough information about the microstructure of the system in order to be able to calculate the variance of the interaction [Eq. (15)].

The system chosen was metallic inclusions in dispersionless gelatin and a Drude dielectric function was used for the metallic part. We presented numerical results for the imaginary part of the effective dielectric tensor $\underline{\epsilon}_M$ as a function of frequency for different combinations of geometrical and structural parameters. The structure of the peaks in this spectra shows that spatial disorder induces an asymmetric broadening along with a coupling of modes with perpendicular polarizations. We remark that this coupling arises in our system even though it has no orientational disorder, and that, since it is absent in the MFA, it is a clear signature of the fluctuations. We believe that the concepts developed in this paper will also prove to be relevant to the calculation of the optical properties of other anisotropic disordered systems such as nematic liquid crystals, in which the distribution functions of the actual microstructure and the disorder-induced field fluctuations have not yet been incorporated.

ACKNOWLEDGMENTS

We are grateful to Cecilia Noguez for her assistance in the numerical work and to J. Récamier for useful discussions. One of us (J.G.) acknowledges the support of Fundación para la Promoción de la Investigación y la Tecnología del Banco de la República (Colombia) and to Instituto de Física de la Universidad Nacional Autónoma de México (México) for its kind hospitality. Two of us (R.G.B. and W.L.M.) acknowledge the support of Dirección General de Asuntos del Personal Académico de la Universidad Nacional Autónoma de México (México) for the support under Contract Nos. IN-104689 and IN-102592.

APPENDIX A

The interaction tensor $s_{ij}^{\gamma\delta}$ is defined as

$$E_i^{\gamma} = s_{ij}^{\gamma\delta} p_j^{\delta} , \tag{A1}$$

where E_i^{γ} is the component of the electric field at $\mathbf{R}_i$ induced by a spheroid at $\mathbf{R}_j$ with a dipole moment p_i^{δ} along the δ direction. The interaction tensor is symmetric in its Cartesian indexes and it depends only on the vector $\mathbf{R}_{ij} \equiv \mathbf{R}_i - \mathbf{R}_j$, that is $s_{ij}^{\gamma\delta} = s_{ij}^{\gamma\delta}(\mathbf{R}_{ij})$, thus here we will omit the indexes i,j and give explicit expressions for $s^{\gamma\delta}(\mathbf{R})$ in prolate (oblate) spheroidal coordinates (ξ,η,ϕ) defined by[12]

$$\begin{aligned} x &= F[(\eta^2 \mp 1)(1-\xi^2)]^{1/2}\cos\phi , \\ y &= F[(\eta^2 \mp 1)(1-\xi^2)]^{1/2}\sin\phi , \\ z &= F\eta\xi , \end{aligned} \tag{A2a}$$

where x,y,z are the Cartesian components and $F = (a_\eta^2 - b_\eta^2)^{1/2}$. The upper (lower) sign used here and later is for the prolate (oblate) spheroidal coordinates. The parameters a_η and b_η are one-half of the distance along the axis of symmetry and either of the two equal axes, respectively, within a spheroidal surface for a given η. The range of the coordinates is

$$\begin{aligned} &1 \le \eta \le \infty \quad (P) , \\ &0 \le \eta \le \infty \quad (O) , \\ &-1 \le \xi \le 1 , \\ &0 \le \phi \le 2\pi . \end{aligned} \tag{A2b}$$

In these coordinates the Cartesian components of the interaction tensor can be written as

$$s^{xx}(\mathbf{R}) = 3(\eta_0/a)^3 \left\{ \frac{\pm\eta}{\eta^2 \mp 1} \left[\frac{1-\xi^2}{\eta^2 \mp \xi^2} \right] \cos^2\phi + \frac{1}{2} Q'_{10}(\eta) \right\} , \tag{A3a}$$

$$s^{xy}(\mathbf{R}) = 3(\eta_0/a)^3 \frac{\pm\eta}{\eta^2 \mp 1} \left[\frac{1-\xi^2}{\eta^2 \mp \xi^2} \right] \cos\phi \sin\phi , \tag{A3b}$$

$$s^{xz}(\mathbf{R}) = 3(\eta_0/a)^3 \frac{\xi}{\eta^2 \mp \xi^2} \left[\frac{1 \mp \xi^2}{\eta^2 \mp 1} \right]^{1/2} \cos\phi , \tag{A3c}$$

$$s^{zz}(\mathbf{R}) = -3(\eta_0/a)^3 \left[Q_0(\eta) - \frac{\eta}{\eta^2 \mp \xi^2} \right] , \tag{A3d}$$

where η_0 is the value of the spheroidal coordinate which defines the surface of the actual spheroidal inclusion,

$$Q_0(\eta) = \begin{cases} \frac{1}{2}\ln\left[\dfrac{\eta+1}{\eta-1} \right] & (P) , \\ \cot^{-1}(\eta) & (O) . \end{cases} \tag{A3e}$$

$Q'_{10}(\eta)$ is the derivative of the associated Legendre polynomial of the second kind,

$$Q_{10}(\eta)=\begin{cases}\frac{1}{2}\eta\ln\left[\dfrac{\eta+1}{\eta-1}\right]-1 & (P)\ ,\\ \eta\cot^{-1}(\eta)-1 & (O)\ ,\end{cases} \tag{A3f}$$

and Q'_{10} satisfies the relation

$$Q_{10}(\eta)=\eta Q'_{10}(\eta)\pm 1/(\eta^2\mp 1)\ . \tag{A4}$$

Since the two equal axes of the spheroid are along the x and y directions, the components of the interaction tensor with y Cartesian components are identical to the ones with x Cartesian components with the replacement of $\cos\phi$ by $\sin\phi$ and vice versa. Also, it is easy to show that at large distances ($\eta\gg 1$), the components of the interaction tensor $s^{\gamma\delta}$ become identical to the ones of the dipole-dipole interaction tensor [Eq. (12)]; this only means that at large distances the electric field induced by a polarized ellipsoid is dipolar.

APPENDIX B

In this appendix we show that, for two-particle distribution functions $\rho^{(2)}(\mathbf{R})$ with spheroidal symmetry, the multipolar contributions to the average of the interaction tensor $\mathcal{L}_\zeta-1$ as defined in Eq. (10) vanish for multipoles higher than the dipole. By spheroidal symmetry we mean that the level surfaces of $\rho^{(2)}$, i.e., those on which $\rho^{(2)}(\mathbf{R})$ is constant, are coaxial spheroids. For prolate spheroids this can be expressed in spherical coordinates as

$$\rho(R,\mu)=\rho(r_<)\ , \tag{B1}$$

where $\mu=\cos\theta$ and θ is the azimuthal angle,

$$r_<=\sqrt{1-e^2(r_<)\mu^2}R \tag{B2}$$

is the small semiaxis of that particular level surface that contains the point (R,μ). Notice that Eq. (B2) is an implicit equation for $r_<$ in the more general case where the eccentricity $e(r_<)$ of the level surfaces depends on $r_<$. First, we perform a multipolar expansion

$$s^{zz}(\mathbf{R})=-\frac{\partial}{\partial z}\sum_{l=1}^{\infty}B_l\frac{P_l(\mu)}{R^{l+1}}=\sum_{l=1}^{\infty}B_l\frac{P_{l+1}}{R^{l+2}}\ , \tag{B3}$$

where B_l are the expansion coefficients and for definitiveness we have chosen $\zeta=z$. Then, to evaluate Eq. (10) we need the integrals

$$I_l=\int d^3R\,\rho^{(2)}(\mathbf{R})\frac{P_{l+1}(\mu)}{R^{l+2}} \tag{B4}$$

for $l\geq 2$. Notice that we omitted the exponential e^{iqz} and the limit $q\to 0$ since for $l\geq 2$ the integrand in Eq. (B4) decays rapidly enough for the integral to be absolutely convergent. The integral corresponding to $l=1$ will be discussed in Appendix C.

Changing variables from R to $r_<$, Eq. (B4) becomes

$$\frac{I_l}{2\pi}=\int_0^{\infty}dr_<\left[1+r_<e(r_<)\frac{de(r_<)}{dr_<}\right]\frac{\rho^{(2)}(r_<)}{r_<^l}\times\int_{-1}^{1}d\mu\,P_{l+1}(\mu)[1-e^2(r_<)\mu^2]^{(l-1)/2}\ . \tag{B5}$$

For l even the angular integral vanishes by symmetry. For odd $l=2n+1$ it also vanishes because its integrand is the product of $P_{2n+2}(\mu)$ times a polynomial of order $2n$ in μ to which it is orthogonal. Similar results can be shown to hold for the angular integral corresponding to oblate spheroids, and for the xx and yy components of the interaction tensor. The result above does not apply to the $l=1$ case since the complex exponential cannot be removed. Therefore, the average of the exact interaction tensor is equal to the average of its dipolar component. This average will be performed explicitly for the simple (HC) distribution function in Appendix C.

APPENDIX C

In this appendix we calculate the average of the interaction tensor $\mathcal{L}_\zeta-1$ as defined in Eq. (10) for the (HC) correlation function

$$\rho^{(2)}_{\mathrm{HC}}(R,\mu)=\Theta(R-r_H(\mu))\ , \tag{C1}$$

where Θ is the unit step function, $\mu=\cos\theta$, θ being the azimuthal angle in spherical coordinates, and $r_H(\mu)=r_{H<}/(1-e_H^2\mu^2)^{1/2}$ ($r_H(\mu)=r_{H>}/[1+g^2(e_H)\mu^2]^{1/2}$) describes the surface of a prolate (oblate) correlation hole with semiaxes $r_{H>}$ and $r_{H<}$ and eccentricity e_H. The function g is defined in Eq. (1f).

As shown in Appendix B, the average might be calculated by considering only the dipolar contribution $t_{ij}^{\gamma\delta}$ to the exact interaction $s_{ij}^{\gamma\delta}$. Using Eqs. (10) and (12) we write

$$\mathcal{L}^z-1=\lim_{q\to 0}\int_0^{\infty}\frac{dR}{R}\int_{-1}^{1}d\mu\,P_2(\mu)e^{iqR\mu}\rho^{(2)}(R,\mu)\ . \tag{C2}$$

Notice that, in contrast to Eq. (B4), in Eq. (C2) we keep the complex exponential since otherwise the integrand would be only conditionally convergent.

One now expands the exponential[24] and $\rho^{(2)}$ in terms of Legendre polynomials:

$$e^{-iqR\mu}=\sum_{l=0}^{\infty}(-i)^l(2l+1)j_l(qR)P_l(\mu)\ , \tag{C3}$$

$$\rho^{(2)}(R,\mu)=\sum_{l=0}^{\infty}\rho_l(R)P_l(\mu)\ , \tag{C4a}$$

where P_l (j_l) is Legendre polynomial (spherical Bessel functions) of order l and

$$\rho_l(R)=\frac{2l+1}{2}\int_{-1}^{1}d\mu\,\rho^{(2)}(R,\mu)P_l(\mu)\ . \tag{C4b}$$

Substituting Eqs. (C3) and (C4) into Eq. (C2), one gets

$$\mathcal{L}_z-1=\lim_{q\to 0}\sum_{l,l'}(-i)^l(2l+1)\times\int_0^{\infty}dR\frac{j_l(qR)}{R}\rho_{l'}(R)\times\int_{-1}^{1}d\mu\,P_2(\mu)P_l(\mu)P_{l'}(\mu)\ . \tag{C5}$$

But we know[25] that

$$\int_{-1}^{1} d\mu\, P_2(\mu) P_l(\mu) P_{l'}(\mu) = \tfrac{2}{5} \langle ll'00|ll'20\rangle^2 , \tag{C6}$$

where $\langle l_1, l_2 m_1 m_2 | l_1 l_2 LM \rangle$ are the Clebsch-Gordan coefficients as given in Ref. 26. Thus, combining Eqs. (C6) and (C5), one can write

$$\mathcal{L}_z - 1 = \lim_{q\to 0} \tfrac{2}{5} \sum_{l,l'} (-i)^l (2l+1) \langle ll'00|ll'20\rangle^2 \times \int_0^\infty dR \frac{j_l(qR)}{R} \rho_{l'}(R) . \tag{C7}$$

Using Eq. (C1) we find the coefficients

$$\rho_l = \begin{cases} 0, & R < r_{H<} , \\ \delta_{l,0} , & R > r_{H>} , \end{cases} \tag{C8a}$$

and for $r_{H<} < R < r_{H>}$,

$$\rho_l(R) = \begin{cases} (2l+1) \int_0^{\mu R} d\mu\, P_l(\mu) \quad (P) , \\ (2l+1) \int_{\mu R}^1 d\mu\, P_l(\mu) \quad (O) , \end{cases} \tag{C8b}$$

where

$$\mu_R = \frac{1}{e_H} \left[1 - \frac{r_{H<}^2}{R^2} \right]^{1/2} \quad (P) \tag{C8c}$$

and

$$\mu_R = \frac{1}{g(e_H)} \left[\frac{r_{H>}^2}{R^2} - 1 \right]^{1/2} \quad (O) . \tag{C8d}$$

Substituting these expression for ρ_l into Eq. (C8) and taking the limit $q \to 0$, we obtain, after some algebra,

$$\mathcal{L}_z = \frac{1}{3} + \int_{r_{H<}}^{r_{H>}} \frac{dR}{R} \mu_R (\mu_R^2 - 1) . \tag{C9}$$

The first term on the right-hand side corresponds to a spherical exclusion hole. The remaining integral can be done by elementary methods and yields

$$\mathcal{L}_z = L_z(e_H) , \tag{C10}$$

where $L_z(e_H)$ is the depolarization factor of a spheroid of eccentricity e_H and is given by Eqs. (1c). For the particular case in which the correlation hole excludes only the volume limited by the overlap of two inclusions, then $e_H = e$ and we obtain Eq. (11).

APPENDIX D

In this appendix we calculate the coefficients $f^{\gamma\delta}$ as defined in Eq. (19). When one writes explicitly the average $\langle \sum_{j\delta} S_{ij}^{\gamma\delta} S_{ji}^{\delta\gamma} \rangle$ in spheroidal coordinates (see Appendix A), for $\rho^{(2)}$ with azimuthal symmetry, Eq. (19) becomes

$$f^{\gamma\delta} = f \frac{6ab^2}{2\pi} F^3 \int\int\int d\eta\, d\xi\, d\phi (\eta^2 \mp \xi^2) \rho^{(2)}(\eta,\xi) \times [S^{\gamma\delta}(\eta,\xi,\phi)]^2 . \tag{D1}$$

Substituting into this equation the explicit expressions for $S^{\gamma\delta}$ [Eq. (A3)] and integrating over ϕ yields

$$f^{\gamma\delta} = 54 f \eta_0 (\eta_0^2 \mp 1) \int\int d\eta\, d\xi\, \rho^{(2)}(\eta,\xi) U^{\gamma\delta}(\eta,\xi) , \tag{D2}$$

where η_0 is the value of the spheroidal coordinate which defines the surface of the actual inclusion, and

$$U^{xx} = \frac{3}{8} \frac{(1-\xi^2)^2}{\eta^2 \mp \xi^2} \frac{\eta^2}{(\eta^2 \mp 1)^2} + \frac{1}{2} \frac{\eta}{\eta^2 \mp 1} (1-\xi^2) Q_{10}(\eta) + (\eta^2 \mp \xi^2) \tfrac{1}{4} Q_{10}^2 , \tag{D3a}$$

$$U^{xy} = \frac{(1-\xi^2)^2}{(\eta^2 \mp \xi^2)} \frac{\eta^2}{(\eta^2 \mp 1)^2} , \tag{D3b}$$

$$U^{xz} = \left[\frac{1-\xi^2}{\eta^2 \mp \xi^2} \right] \frac{\xi^2}{\eta^2 \mp 1} , \tag{D3c}$$

$$U^{zz} = (\eta^2 \mp \xi^2) \left[Q_0(\eta) - \frac{\eta}{\eta^2 \mp \xi^2} \right]^2 . \tag{D3d}$$

For $\rho^{(2)}$ we now choose $\rho_{\rm HC}^{(2)}$ as defined in Eq. (C1). After expressing $\rho_{\rm HC}^{(2)}$ in spheroidal coordinates one gets

$$f^{\gamma\delta} = 54 f \eta_0 (\eta_0^2 \mp 1) \left[2 \int_{\eta_1}^{\eta_2} d\eta \int_0^{\xi 1(\eta)} d\xi\, U^{\gamma\delta}(\eta,\xi) + 2 \int_{\eta_2}^{\infty} d\eta \int_0^1 d\xi\, U^{\gamma\delta}(\eta,\xi) \right] , \tag{D4a}$$

where

$$\eta_1 = \begin{cases} 2\eta_0 (1 - 3/4\eta_0^2)^{1/2} \quad (P) , \\ 2\eta_0 \quad (O) , \end{cases} \tag{D4b}$$

$$\eta_2 = \begin{cases} 2\eta_0 \quad (P) , \\ 2\eta_0 (1 + 3/4\eta_0)^{1/2} \quad (O) , \end{cases} \tag{D4c}$$

$$\xi_1^2(\eta) = \eta_0^2 \frac{3 \mp 4\eta_0^2 \pm \eta^2}{\eta^2 \mp \eta_0^2} . \tag{D4d}$$

One is able, then, to perform the integrals over ξ analytically, leading to

$$f^{\gamma\delta} = 54 f \eta_0 (\eta_0^2 \mp 1) C^{\gamma\delta} \left[\int_{\eta_1}^{\eta_2} d\eta\, V^{\gamma\delta}[\eta, \xi_1(\eta)] + \int_{\eta_2}^{\infty} d\eta\, V^{\gamma\delta}[\eta, \xi_1(\eta_2)] \right] , \tag{D5a}$$

where

$$C_{zz} = C_{xx} = 2 , C_{zx} = 1 , \quad C_{xy} = \tfrac{1}{4} , \tag{D5b}$$

$$V^{xx}(\eta,\xi_1) = \frac{3}{8} \frac{\eta^2}{(\eta^2 \mp 1)^2} \left[W_0(\xi_1) - 2W_2(\xi_1) + W_4(\xi_1) \right] \pm \frac{1}{2} \frac{\eta}{\eta^2 \mp 1} Q_{10}' \left[u - \frac{u^3}{3} \right] + \tfrac{1}{4} (Q_{10}')^2 \left[\eta^2 u - \frac{u^3}{3} \right] , \tag{D5c}$$

$$V^{xy}(\eta,\xi_1)=\frac{\eta^2}{(\eta^2\mp1)^2}[W_0(\xi_1)-2W_2(\xi_1)+W_4(\xi_1)]\ , \tag{D5d}$$

$$V^{xz}(\eta,\xi_1)=\frac{1}{\eta^2\mp1}\left[W_2(\xi_1)-W_4(\xi_1)\right]\ , \tag{D5e}$$

$$V^{zz}(\eta,\xi_1)=Q_0^2\left[\eta^2u\mp\frac{u^3}{3}\right]-2Q_0\eta u+\eta^2W_0(\xi_1)\ . \tag{D5f}$$

Equation (D5a) is the same as Eq. (20) where we identify $Q^{\gamma\delta}$ with the expression within square brackets. In these expressions

$$u=\begin{cases}\xi_1\ , \\ 1-\xi_1\ ,\end{cases} \tag{D5g}$$

$$W_0(\xi_1)=\begin{cases}\frac{1}{\eta}\frac{1}{2}\ln\frac{\eta+\xi_1}{\eta-\xi_1}\ , \\ \frac{1}{\eta}\tan^{-1}\left[\frac{1}{\eta}\right]-\frac{1}{\eta}\tan^{-1}\left[\frac{\xi_1}{\eta}\right]\ ,\end{cases} \tag{D5h}$$

$$W_2(\xi_1)=\begin{cases}-\xi_1+\eta^2W_0(\xi_1)\ , \\ (1-\xi_1)-\eta^2W_0(\xi_1)\ ,\end{cases} \tag{D5i}$$

$$W_4(\xi_1)=\begin{cases}-\frac{\xi_1^3}{3}+\eta^2W_2(\xi_1)\ , \\ \frac{(1-\xi_1)^3}{3}-\eta^2W_2(\xi_1)\ ,\end{cases} \tag{D5j}$$

where the formulas above (below) correspond to prolate (oblate) spheroidal inclusions.

APPENDIX E

Assuming the hole correction [Eq. (C1)] for the two-particle distribution function, we calculate here the coefficients $f^{\gamma\delta}$ required in Eq. (18), when the dipole-dipole interaction tensor $t_{ij}^{\gamma\delta}$ [Eq. (12)] is used instead of $s_{ij}^{\gamma\delta}$ [Eq. (A3)]. Their definition is given in Eq. (19) which becomes

$$\tfrac{1}{4}f^{\gamma\delta}=(ab^2)^2\left\langle\sum_j t_{ij}^{\gamma\delta}t_{ji}^{\delta\gamma}\right\rangle\ . \tag{E1}$$

When $t_{ij}^{\gamma\delta}$ is substituted from Eq. (12) into this equation and the ensemble average is calculated for a system with azimuthal symmetry, one gets, in spherical coordinates,

$$\tfrac{1}{4}f^{\gamma\delta}=\tfrac{3}{2}ab^2f\int_0^\infty dR\int_{-1}^{1}d\mu\frac{1}{R^4}\rho^{(2)}(R,\mu)H^{\gamma\delta}(\mu)\ , \tag{E2}$$

where $\mu\equiv\cos\theta$ and

$$H^{\gamma\delta}(\mu)=\frac{1}{2\pi}\int_0^{2\pi}d\phi\,\hat{\mathbf{e}}^{\gamma}\cdot(3\hat{\mathbf{R}}\hat{\mathbf{R}}-\underline{1})\cdot\hat{\mathbf{e}}^{\delta}\hat{\mathbf{e}}^{\delta}\times(3\hat{\mathbf{R}}\hat{\mathbf{R}}-\underline{1})\cdot\hat{\mathbf{e}}^{\gamma}\ . \tag{E3}$$

Here $\hat{\mathbf{e}}^{\gamma}$ ($\gamma=x,y,z$) are the unit vectors along the Cartesian axes and $\hat{\mathbf{R}}=\mathbf{R}/R$. Using this definition and performing the integrals over ϕ, one is able to write

$$H^{\gamma\delta}(\mu)=\sum_{l=0}^{2}h_{2l}^{\gamma\delta}P_{2l}(\mu)\ , \tag{E4a}$$

where $P_l(\mu)$ are the Legendre polynomials of order l and

$$h_0^{xx}=h_0^{zz}=\tfrac{4}{5}\ ,\quad h_0^{xy}=h_0^{xz}=\tfrac{3}{5}\ , \tag{E4b}$$

$$h_2^{xx}=-\tfrac{4}{7}\ ,\quad h_2^{zz}=\tfrac{8}{7}\ ,\quad h_2^{xy}=-\tfrac{6}{7}\ ,\quad h_2^{xz}=\tfrac{3}{7}\ , \tag{E4c}$$

$$h_4^{xx}=\tfrac{27}{35}\ ,\quad h_4^{zz}=\tfrac{72}{35}\quad h_4^{xy}=\tfrac{9}{35}\ ,\quad h_4^{xz}=-\tfrac{36}{35}\ . \tag{E4d}$$

One now expands $\rho^{(2)}$ in Legendre polynomials, as it was done in Eq. (C4), and substitutes it in the integrand of Eq. (E2). Then, after performing the integration over μ, one obtains

$$\tfrac{1}{4}f^{\gamma\delta}=\tfrac{3}{2}ab^2f\sum_{l=0}^{2}\frac{2}{4l+1}h_{2l}^{\gamma\delta}\int_0^\infty\frac{1}{R^4}\rho_{2l}(R)dR\ , \tag{E5}$$

where the harmonic coefficients ρ_{2l} are defined by Eq. (C4b). At this point one chooses for $\rho^{(2)}$ the hole correction $\rho_{\rm HC}^{(2)}$, defined by Eq. (C1), and substitutes its harmonic coefficients, as given by Eqs. (C8), into the integrand of Eq. (E5) in order to obtain, after some algebra,

$$f^{\gamma\delta}=f_0^{\gamma\delta}+\frac{3}{4}\left[\frac{a}{b}\right]fd^2\sum_{l=0}^{2}h_{2l}^{\gamma\delta}I_{2l}\ , \tag{E6a}$$

where

$$f_0^{\gamma\delta}=\tfrac{1}{2}fh_0^{\gamma\delta}\times\begin{cases}(b/a)^2\ \ (P)\ , \\ a/b\ \ \ (O)\ ,\end{cases} \tag{E6b}$$

$$I_0=\begin{cases}2T_2\ \ (P)\ , \\ -2(T_2-T_1)\ \ (O)\ ,\end{cases} \tag{E6c}$$

$$I_2=\pm(T_4-T_2)\ , \tag{E6d}$$

$$I_4=\pm\tfrac{1}{4}(7T_6-10T_4+3T_2)\ . \tag{E6e}$$

Here d is equal to the eccentricity e or to $g(e)$, as defined in Eq. (1e), depending on whether the spheroidal inclusions are prolate or oblate, respectively,

$$T_n=\int_0^1x^nv(x)dx\ , \tag{E6f}$$

$$v(x)=(1\mp d^2x^2)^{1/2}\ , \tag{E6g}$$

and the upper (lower) sign is for prolate (oblate) spheroidal inclusions. This convention will be also followed in the expressions below. The integrals T_n are tabulated[27] and are given by

$$T_1=\frac{1}{3}\frac{(b/a)^3-1}{g^2(e)}\quad\text{(oblate only)}\ , \tag{E7a}$$

$$T_2=\pm\frac{1}{8d^2}\left[v_1+\frac{\beta}{d}-2v_1^3\right]\ , \tag{E7b}$$

$$T_4=\pm\frac{1}{2d^2}\left[T_2-\frac{v_1^3}{3}\right]\ , \tag{E7c}$$

$$T_6=\pm\frac{1}{2}\left[T_4-\frac{v_1^3}{5}\right]\ , \tag{E7d}$$

where $\beta=\sin^{-1}(e)$ or $\ln[g(e)+v_1]$ for prolate or oblate spheroids, respectively, and $v_1=(1\mp d^2)^{1/2}$.

[1]A review of the early history of this subject is given by R. Landauer, in *Electrical Transport and Optical Properties of Inhomogeneous Media (Ohio State University, 1977),* Proceedings of the First Conference on the Electrical Transport and Optical Properties of Inhomogeneous Media, AIP Conf. Proc. No. 40, edited by J. C. Garland and D. B. Tanner (AIP, New York, 1978), p. 2.

[2]See, for example, N. E. Cusack, *The Physics of Structurally Disordered Matter* (Hilger, Bristol, 1987).

[3]G. A. Niklasson and C. G. Granqvist, in *Contribution of Cluster Physics to Materials Science and Technology,* Vol. 104 of NATO Advanced Study Institute, edited by J. Davenas and P. M. Rabette (Nijhoff, Dordrecht, 1986), p. 539.

[4]P. N. Sen, C. Scala, and M. H. Cohen, Geophys. **46**, 781 (1981), and references therein; L. C. Sheu, C. Liu, J. Korringa, and K. J. Dunn, J. Appl. Phys. **67**, 7071 (1990).

[5]K. Asami, T. Hanai, and N. Koizumi, Jpn. J. Appl. Phys. **19**, 359 (1980); J. M. Tean, C. K. Chan, G. R. Flemming, and T. Gowens, Biophys. J. **56**, 1203 (1989); J. O. Brönander, P. Apell, and T. Gillbro (unpublished).

[6]See, for example R. Landauer, *Electrical Transport and Optical Properties of Inhomogeneous Media* (Ref. 1); G. A. Niklasson and C. G. Granqvist, *Contribution of Cluster Physics to Materials Science and Technology* (Ref. 3). See (a) *Physics and Chemistry of Porous Media (Schlumberger-Doll Research, Ridgefield Connecticut),* Proceedings of the Symposium on the Physics and Chemistry of Porous Media, AIP Conf. Proc. No. 407, edited by D. L. Johnson and P. N. Sen (AIP, New York, 1984); (b) *Electrodynamics of Interfaces and Composite Systems,* edited by R. G. Barrera and W. L. Mochán (World Scientific, Singapore, 1988); (c) *Thin Films and Small Particles,* edited by M. Cardona and J. Giraldo (World Scientific, Singapore, 1989); (d) J. Lafait and D. B. Tanner, Physica A **157** (1990).

[7]See, for example, R. G. Barrera, G. Monsivais, W. L. Mochán, and E. Anda, Phys. Rev. B **39**, 9998 (1989), and references therein.

[8]J. C. Maxwell Garnett, Philos. Trans. R. Soc. London **203**, 385 (1904); **205**, 237 (1906).

[9]See, for example, J. D. Jackson, *Classical Electrodynamics,* 2nd ed. (Wiley, New York, 1975), p. 155.

[10]H. A. Lorentz, *The Theory of Electrons* (Dover, New York, 1952); Ann. Phys. Chem. **9**, 641 (1880).

[11]J. C. Maxwell, *A Treatise on Electricity and Magnetism* (Dover, New York, 1954), Vol. I, Sec. 354.

[12]D. S. Wang and M. Kerker, Phys. Rev. B **24**, 1777 (1981).

[13]C. F. Bohren and D. R. Hoffman, *Absorption and Scattering of Light by Small Particles* (Wiley, New York, 1957), Sec. 5.3.

[14]O. Wiener, Abh. Math. Phys. Sächs. Ges. Wiss. **32**, 509 (1912).

[15]W. L. Bragg and A. B. Pippard, Acta Crystallogr. **6**, 865 (1953).

[16]R. W. Cohen, G. D. Cody, M. D. Couts, and B. Abeles, Phys. Rev. B **8**, 3689 (1973).

[17]F. L. Galeener, Phys. Rev. Lett. **27**, 421 (1971).

[18]G. B. Smith, Appl. Phys. Lett. **35**, 668 (1979).

[19]G. A. Niklasson and C. G. Granquist, J. Appl. Phys. **55**, 3382 (1984).

[20]R. G. Barrera, G. Monsivais, and W. L. Mochán, Phys. Rev. B **38**, 5371 (1988).

[21]Lev M. Blinov, *Electro-Optical and Magneto-Optical Properties of Liquid Crystals* (Wiley, New York, 1983), Chap. 2, and references therein.

[22]H. E. J. Neugebauer, Can. J. Phys. **28**, 292 (1950); **32**, 1 (1954); A. Saupe and W. Maier, Z. Naturforsch. Teil A **16**, 816 (1961); M. F. Vuks, Opt. Spectrosc. **20**, 361 (1966); W. Maier and G. Meier, Z. Naturforsch. Teil. A **18**, 262 (1961); D. A. Dunmur, Chem. Phys. Lett. **10**, 49 (1971); P. G. Cummins, D. A. Dunmur, and D. A. Laidler, Mol. Cryst. Liq. Cryst. **30**, 109 (1975).

[23]J. G. Kirkwood, J. Chem. Phys. **4**, 592 (1936).

[24]E. Merzbacher, *Quantum Mechanics* (Wiley, New York, 1963), p. 207.

[25]*Handbook of Mathematical Functions,* edited by M. Abramowitz and I. A. Stegun (Dover, New York, 1970), p. 514.

[26]E. V. Condon and G. N. Shortley, *The Theory of Atomic Spectra* (Cambridge University Press, Cambridge, 1964), p. 75.

[27]I. S. Gradshteyn and I. M. Ryzhik, *Table of Integrals, Series and Products* (Academic, New York, 1980).